

Experimental signals of σ -mesons in nuclei and chiral symmetry

M.J. Vicente Vacas^a

Departamento de Física Teórica and IFIC, Universidad de Valencia-CSIC, Ap. Correos 22085, E-46071 Valencia, Spain

Received: 30 September 2002 /

Published online: 22 October 2003 – © Società Italiana di Fisica / Springer-Verlag 2003

Abstract. The $\pi\pi$ interaction in the scalar isoscalar channel is studied as a function of the baryonic density in the framework of a chiral unitary approach which successfully reproduces vacuum π - π phase shifts. We present some results on the σ -meson pole, which is generated dynamically in our model, in nuclear matter. Finally, we analyze the $(\gamma, \pi\pi)$ reaction on nucleons and nuclei in the kinematical region where the scalar isoscalar $\pi\pi$ scattering amplitude is influenced by the low mass of the σ in nuclei, and thus, presents a large enhancement close to the position of its pole. Indeed, we find, that the final-state interaction of the pions modified by the nuclear medium produces a large shift of strength of the two-pion invariant-mass distribution in the $(\gamma, \pi^0\pi^0)$ channel consistent with recent experimental data.

PACS. 14.40.-n Properties of specific particles: Mesons – 25.20.-x Photonuclear reactions – 21.65.+f Nuclear matter

1 Introduction

In the past years, much effort has been devoted to the study of the $\pi\pi$ scattering amplitude in nuclei and its possible experimental signals, like the enhancement of the $\pi\pi$ invariant-mass distributions close to the $\pi\pi$ threshold, seen in the experiments of pion-induced two-pion production in nuclei [1], and the large strength shift found in the $(\pi, \pi^0\pi^0)$ process [2].

The idea of strong threshold effects due to the $\pi\pi$ interaction in a dense nuclear medium was first suggested in ref. [3]. These effects would show up in the scalar-isoscalar $-\sigma-$ channel and could be interpreted as due to a drop of the σ mass in nuclear matter. Later works, paying attention to the chiral constraints of the $\pi\pi$ amplitude and trying to use realistic potentials, found indeed an appreciable enhancement of the $\pi\pi$ scattering amplitude close to threshold [4–7].

These theoretical $\pi\pi$ scattering amplitudes in the nuclear medium have been used in the analysis of the $(\pi, \pi\pi)$ reactions in nuclei [8–10]. Although the modifications of the $\pi\pi$ invariant-mass distributions produced by the $\pi\pi$ scattering go in the right direction, the calculations have not been successful in fully reproducing the medium effects found in the experiment. A much better agreement has been obtained in the case of the $(\gamma, \pi\pi)$ reaction [11, 12], which has the obvious advantage of exploring higher nuclear densities. Additionally, the $N(\gamma, \pi\pi)N$ scattering amplitude is simpler and does not have the strong interference between different mechanisms that occurs in the elementary $\pi N \rightarrow (\pi\pi)_{I=0}N$ reaction.



Fig. 1. Terms of the meson-meson scattering amplitude accounting for ph and Δh excitation.

In this paper, we will present briefly our results on the in-medium $\pi\pi$ interaction in the s -wave, $I = 0$ channel. We will consider the σ pole dependence on the nuclear density and finally, we will discuss the experimental signature of these medium effects in the $(\gamma, \pi\pi)$ reaction.

2 σ -meson in the medium

2.1 $\pi\pi$ interaction and the σ pole

The pion pion interaction in nuclear matter has been calculated in the framework of a chiral unitary approach which generates the f_0 - and σ -resonances and reproduces well the meson-meson phase shifts in vacuum. The pions undergo multiple scattering which is accounted for by means of the Bethe-Salpeter equation,

$$T = V + VG_{\pi\pi}T, \quad (1)$$

where V is given by the lowest-order chiral amplitude for $\pi\pi \rightarrow \pi\pi$ in s -wave and $I = 0$, and $G_{\pi\pi}$ is the loop function of the two-pion propagators properly renormalized. The nuclear medium effects are basically driven by the attractive p -wave pion self-energy, represented by the particle-hole bubbles in fig. 1, and are incorporated by

^a e-mail: Manuel.J.Vicente@uv.es

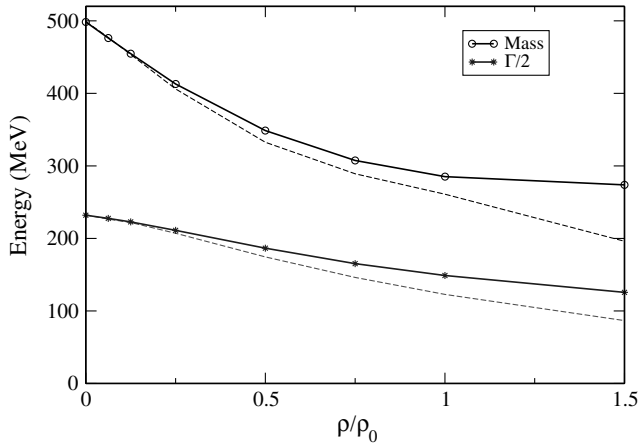


Fig. 2. σ mass and half-width as a function of the density. Dashed lines include also the $2ph$ pion self-energy pieces.

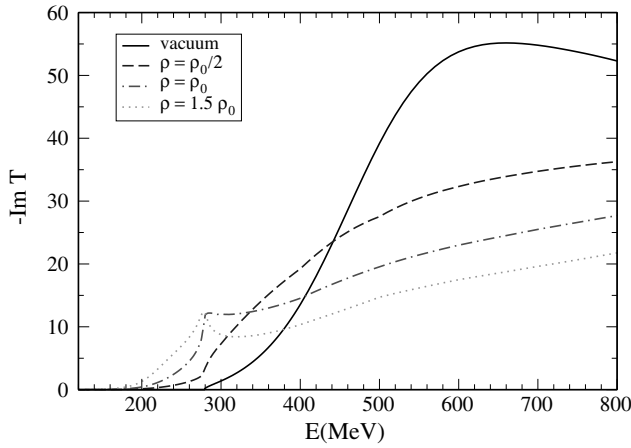


Fig. 3. Imaginary part of the $\pi\pi$ scattering amplitude at several densities.

modifying the pion propagators and including new pieces in the Bethe-Salpeter equation. Some of these pieces are shown in fig. 1. Full details of the calculation can be found in refs. [6] and [13].

In fig. 2, we present our results for the σ mass and its width as a function of the baryon density [13]. We find that both mass and width decrease as the density increases, reaching a mass around 250 MeV and a similar width at 1.5 times the nuclear density. Even at intermediate densities the σ pole is close to the 2π threshold. The influence of this pole is clear over the real energy axis and produces a peak in the $\pi\pi$ scattering amplitude at low energies as can be seen in fig. 3. The accumulation of strength depends quite strongly on the density, and therefore one should not expect any dramatic enhancement in peripheral reactions like $A(\pi, \pi\pi)X$.

2.2 The $A(\gamma, \pi\pi)X$ reaction

In contrast with the $(\pi, \pi\pi)$ reactions, the photon beam is not strongly distorted, and two-pion photoproduction probes deeper regions of the nuclei. For the elementary

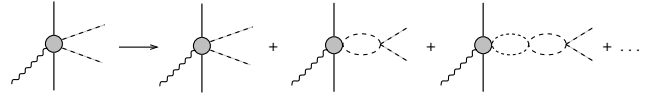


Fig. 4. Diagrammatic series for pion final-state interaction in $I = 0$.

$(\gamma, \pi\pi)$ reaction we follow the model of ref. [14] which couples the photons to mesons, nucleons and the resonances $\Delta(1232)$, $N^*(1440)$, $N^*(1520)$ and $\Delta(1700)$. This model reproduces all the charge channels at low energies well. Final-state interaction of the πN system is accounted for by means of the explicit use of resonances with their widths.

The two final pions undergo multiple scattering which can be accounted for by means of the Bethe-Salpeter equation as shown diagrammatically in fig. 4.

The two-pion final-state interaction is incorporated in the $I = 0$ part of the $(\gamma, \pi\pi)$ amplitude by factorizing the on-shell tree level $\gamma N \rightarrow \pi\pi N$ and $\pi\pi \rightarrow \pi\pi$ amplitudes in the loop functions:

$$T_{(\gamma, \pi^0 \pi^0)}^{I_{\pi\pi}=0} \longrightarrow T_{(\gamma, \pi^0 \pi^0)}^{I_{\pi\pi}=0} (1 + G_{\pi\pi} t_{\pi\pi}^{I=0}(M_I)), \quad (2)$$

where $G_{\pi\pi}$ is the loop function of the two-pion propagators, which appears in the Bethe-Salpeter equation, and $T_{\pi\pi}^{I=0}$ is the $\pi\pi$ scattering matrix in isospin $I = 0$, taken from ref. [6].

In fig. 5, we can see the results for the invariant-mass distribution of the two pions for hydrogen, ^{12}C and ^{208}Pb . Apart from the in-medium $\pi\pi$ interaction, other nuclear effects like the nucleons Fermi motion and Pauli blocking and the final pion distortion (absorption + quasielastic scattering) have been included in the calculation. That these other effects are well under control can be seen in the right panels showing the reactions $(\gamma, \pi^+\pi^0)$ and $(\gamma, \pi^-\pi^0)$. In this case the two pions have isospin one or two and therefore interact weakly at these low energies. Our calculation incorporating the elementary $\gamma N \rightarrow \pi\pi N$ and the quoted trivial nuclear effects agrees well with the experiment.

On the other hand, as one can see in the figure, there is an appreciable shift of strength to the low invariant-mass region due to the in medium $\pi\pi$ interaction in the $\pi^0\pi^0$ channel. Whereas in hydrogen the distribution peaks around 340 MeV, in nuclei the peak moves towards the 2π threshold. This shift is also well reproduced by our calculation.

These results show a clear signature of the modified $\pi\pi$ interaction in the medium. The fact that the photons are not distorted has certainly an advantage over the pion-induced reactions and allows one to see inner parts of the nucleus. In this sense, it is worth noting that, from our calculations, we can determine the average nuclear density felt by the reaction which turns out to be 35% and 65% of the normal nuclear density for ^{12}C and ^{208}Pb , respectively.

Although we have been mostly discussing this reaction in terms of the $\pi\pi$ interaction in the nuclear medium, its relation to the modification of the σ -meson in the medium

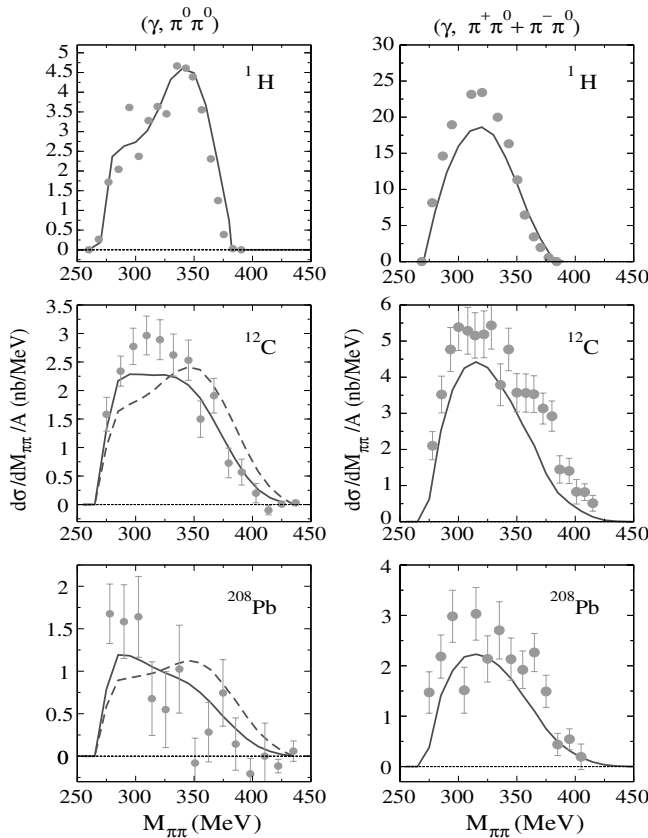


Fig. 5. 2π invariant-mass distribution for the $(\gamma, \pi\pi)$ reaction in hydrogen, ^{12}C and ^{208}Pb . Solid lines: full model including medium final $\pi\pi$ interaction. Dashed lines: idem using vacuum $\pi\pi$ interaction. Experimental data from [11].

is clear. We have mentioned that the reason for the shift of strength to lower invariant masses in the mass distribution is due to the accumulated strength in the scalar isoscalar $\pi\pi$ amplitude in the medium. Yet, this strength is mostly governed by the presence of the σ pole.

3 Conclusions

Present experimental data on both $(\pi, 2\pi)$ and $(\gamma, 2\pi)$ processes seem to confirm the importance of the 2π final state interaction in the scalar-isoscalar —“ σ ”— channel. In our approach, which is based on a conventional many-body

expansion beginning with the standard chiral Lagrangians, the σ -meson both in the free space and in the nucleus is generated dynamically. Studying the evolution of the σ poles as a function of the nuclear density we find that the pole position of the σ moves to smaller energies as the density increases and produces as a consequence some accumulation of strength in the $\pi\pi$ interaction close to threshold.

Using this model, we are able to reproduce the experimental results of the $(\gamma, 2\pi)$ reaction from hydrogen to lead. Given that the $(\pi, 2\pi)$ reaction is more peripheral, and therefore sensitive to lower densities we expect the effects of the final-state interaction to be smaller in this case, what calls for some additional mechanism that could explain the large enhancements found experimentally.

References

1. CHAOS Collaboration (F. Bonutti *et al.*), Phys. Rev. Lett. **77**, 603 (1996); Nucl. Phys. A **638**, 729 (1998); P. Camerini, N. Grion, R. Rui, D. Vetterli, Nucl. Phys. A **552**, 451 (1993); **572**, 791 (1993)(E); F. Bonutti *et al.* (CHAOS Collaboration), Phys. Rev. C **60**, 018201 (1999).
2. Crystal Ball Collaboration (A. Starostin *et al.*), Phys. Rev. Lett. **85**, 5539 (2000).
3. P. Schuck, W. Norenberg, G. Chanfray, Z. Phys. A **330**, 119 (1988).
4. R. Rapp, J.W. Durso, J. Wambach, Nucl. Phys. A **596**, 436 (1996).
5. Z. Aouissat, R. Rapp, G. Chanfray, P. Schuck, J. Wambach, Nucl. Phys. A **581**, 471 (1995).
6. H.C. Chiang, E. Oset, M.J. Vicente Vacas, Nucl. Phys. A **644**, 77 (1998).
7. M.J. Vicente Vacas, E. Oset, H.C. Chiang, Acta Phys. Pol. B **29**, 3137 (1998).
8. R. Rapp *et al.*, Phys. Rev. C **59**, 1237 (1999).
9. M.J. Vicente Vacas, E. Oset, Phys. Rev. C **60**, 064621 (1999).
10. M.J. Vicente Vacas, E. Oset, arXiv:nucl-th/0002010.
11. J.G. Messchendorp *et al.*, Phys. Rev. Lett. **89**, 222302 (2002), arXiv:nucl-ex/0205009.
12. L. Roca, E. Oset, M.J. Vicente Vacas, Phys. Lett. B **541**, 77 (2002), arXiv:nucl-th/0201054.
13. M.J. Vicente Vacas, E. Oset, arXiv:nucl-th/0204055.
14. J.C. Nacher, E. Oset, M.J. Vicente Vacas, L. Roca, Nucl. Phys. A **695**, 295 (2001), arXiv:nucl-th/0012065.